IOP Publishing Physica Scripta
Phys. Scr. 95 (2020) 044007 (12pp) https://doi.org/10.1088/1402-4896/ab6797

Preparation and magneto-optical behavior of ferrofluids with anisometric particles

S N Lysenko[1], A V Lebedev[2], S A Astaf'eva[1], D E Yakusheva[1], M Balasoiu[3,4,5], A I Kuklin[4,5], Yu S Kovalev[4] and V A Turchenko[4,6,7]

[1] Institute of Technical Chemistry, Perm Federal Research Center, Ural Branch, Russian Academy of Sciences, Perm, Russia
[2] Institute of Continuous Media Mechanics, Perm Federal Research Center, Ural Branch, Russian Academy of Sciences, Perm, Russia
[3] Horia Hulubei National Institute for R&D in Physics and Nuclear Engineering, Str. Reactorului no.30, PO Box MG-6, Bucharest-Magurele, Romania
[4] Joint Institute of Nuclear Research, 6 Joliot-Curie St, Dubna, Moscow Region, 141980, Russia
[5] Moscow Institute of Physics and Technology, 9 Institutskiy per., Dolgoprudny, Moscow Region, 141701, Russia
[6] South Ural State University, 76, Lenin Aven., Chelyabinsk, 454080, Russia
[7] Donetsk Institute of Physics and Technology Named after O.O. Galkin of the NASU, 46, Nauki Ave, Kiev, 03680, Ukraine

E-mail: svetlana-astafeva@yandex.ru

Received 20 September 2019, revised 22 December 2019
Accepted for publication 3 January 2020
Published 14 February 2020

Abstract

Nanoparticles of barium hexaferrite have been synthesized by hydrothermal method. Copper and cobalt ferrite nanoparticles have been prepared via a novel coprecipitation technique. The particles were characterized by scanning electron microscopy, transmission electron microscopy, dynamic light scattering, magnetic granulometry, wide angle x-ray diffraction, small angle x-ray scattering, small angle neutron scattering. For preparation of the ferrofluids, relatively large nanoplates have been stabilized by a double layer. A stabilization method has been developed and the stable ferrofluids with large particles have been obtained. Magneto-optical effects in the ferrofluids containing both spherical and anisometric ferrite nanoparticles have been studied. The ferrofluids with relatively large nanoplates—61 and 51 nm—have been found to be efficient magneto-optical media. Magneto-optical response in these media has been shown to be one or two orders of magnitude higher, than the one in the colloids with particle size about 10 nm. Characteristic frequencies and aggregate sizes have been determined using experimental data.

Keywords: ferrites, nanoplates, hydrothermal synthesis, coprecipitation method, ferrofluids, magneto-optical response, small angle neutron scattering

(Some figures may appear in colour only in the online journal)

1. Introduction

Ferrite nanoparticles exhibit amazing magnetic, electrical, dielectric, and microwave properties. These nanoscale objects have attracted an increasing interest in the past decade in the field of nanoelectronics, energy storage, medicine, high-density recording media, electromagnetic interference shielding, catalysis, wastewater treatment etc [1–3]. Magnetic particles are of considerable interest, as their magnetism enables remote excitation by magnetic fields as well as recording of the response by flux sensors of various types. Their static and dynamical properties provide the physical basis for a broad range of technologies in medical diagnostics and therapy [4], magnetic particle based volumetric biosensors [5] and magnetic bead-assisted microrheology [6–8].

Magnetic fluids, or ferrofluids, are the colloids of magnetic nanoparticles in a liquid medium. The size of the nanoparticles is usually about 10 nm, and in a colloid magnetic core is stabilized by surfactants, the most common being oleic acid. Owing to the combination of fluidity of the

medium and magnetic properties of the particles, magnetic fluids have been extensively studied for many years. When a ferrofluid is subjected to external magnetic field, the chain-like aggregates are formed along the field direction. This field-induced structure is characterized by excellent optical properties, such as tunable refractive index, thermal lens effect, magnetochromatics, magneto-optical effect, nonlinear optical effect, birefringence [9–12].

In all applications of the magnetic fluids, the particle size remains the most important parameter, as many of the chemical and physical properties associated to nanoparticles are strongly dependent on the nanoparticle shape and diameter [13]. So numerous microscopic and spectroscopic methods are used for characterization of the particles, often in combination, for more detailed description of the particle shape, size, composition, morphology and core–shell structure.

The physical properties of ferrites depend on their composition, morphology and particle size, which are largely determined by synthetic method. At present the following synthetic methods are used for preparation of nanosized ferrites: solid-phase reactions, mechanical grinding, thermal decomposition of metal acetylacetonates, hydrothermal methods [1, 14, 15], coprecipitation, citrate sol–gel process, thermal decomposition of metal carboxylates, microemulsion method.

Among these synthetic approaches, the hydrothermal process can be distinguished as a low-temperature synthetic method for nanocrystalline spinel ferrite particles. Coprecipitation is also relatively simple method, although it often requires calcination as a final ferritization stage. The nanoparticles obtained by coprecipitation are usually characterized by a homogeneous composition, predetermined stoichiometry and narrow size distribution [16].

In present study, a number of ferrofluids, based on divalent metal ferrite particles and hydrocarbon or aqueous media were synthesized. The particles were characterized by different methods, magneto-optical behavior of the ferrofluids was studied and the physical background of magneto-optical properties was described.

In this paper, preparation of both nanoparticles and ferrofluids, as well as the instruments, used for characterization of the particles and magneto-optical response, are described in the section 'Methods'. The section 'Results and discussion' includes theoretical description of magneto-optical phenomenon, the scheme of the device designed for magneto-optical measurements and discussion of experimental data obtained for a number of ferrofluids. In addition, characterization of the ferrofluid with 'large' nanoplates by small-angle x-ray and neutron scattering methods is given. In the last part of this section the novelty of present study is discussed. The main results, conclusions, and future research trends are presented in the section 'Conclusion'.

2. Methods

2.1. Preparation of barium hexaferrite

Barium hexaferrite nanoplates were prepared according to the hydrothermal procedure described in [17, 18]. Initial aqueous solution with concentrations of 0.05M ferric nitrate $Fe(NO_3)_3$ and 0.01M barium nitrate $Ba(NO_3)_2$ was prepared. 40 ml of 2.72 N alkali solution was added to 40 ml of initial salt solution at vigorous stirring. The resulting suspension of $Fe(OH)_3$ iron hydroxide in a strongly alkaline medium was placed into an autoclave. The reaction mixture was heated to 160 °C at a heating rate of 3 °C min^{-1}, kept at this temperature for 2 h, cooled to 100 °C, then removed from an oven and cooled to room temperature.

2.2. Preparation of copper and cobalt ferrites

Coprecipitation method was used for preparation of copper and cobalt ferrites. The novelty of our variant of coprecipitation method lies in the type of the oxidant used for transformation of Fe (II) to Fe (III), relatively low temperature and a short reaction time.

For preparation of initial solution, 5.6 g (20 mmol) of iron sulfate heptahydrate $FeSO_4 \cdot 7H_2O$, 2.75 g (11 mmol) of copper sulfate pentahydrate $CuSO_4 \cdot 5H_2O$ and 0.84 g (5 mmol) hydroxylamine sulfate $(NH_2OH)_2 \cdot H_2SO_4$ were dissolved in 25 ml of deionized water. Hydroxylamine sulfate was added for oxidation of Fe (II) to Fe (III). Then 4.5 g of an alkali solution with concentration of 8.88 mmol g^{-1} (40 mmol NaOH) was added at vigorous stirring until a brown precipitate was formed. The reaction mixture was heated up to the boiling point at stirring and the second portion of the alkali solution was added (6.75 g, or 60 mmol NaOH). The resulting mixture was heated and boiled for 10 min. Upon boiling the precipitate was washed with water to pH = 8, then concentrated hydrochloric acid was added dropwise until constant pH = 4 was achieved. For neutral medium, the precipitate was washed several times with deionized water. A black precipitate was separated using a magnet.

The same procedure was used for preparation of cobalt ferrite.

2.3. Preparation of ferrofluids

In case of barium hexaferrite, two variants of preparation method were described in [17]. In this work, to obtain a stable colloid, the particles were treated by a common surfactant used for stabilization of ferrofluids—oleic acid. The order of surfactant addition, before or after hydrothermal process, was shown to be rather important in terms of resulting particle size. If oleic acid is added before heating, only fine particles are obtained (see *Ferrofluid 1)*. If it is added upon heating, the particle size distribution is much broader. So, in [17] the authors could not obtain a colloid in the second case (see *Ferrofluid 3*). Here we use the definitions 'small' and 'large' nanoplates to make difference between the particles of the size 10 and 50–60 nm, as these two types of particles are characterized by different behavior in a colloid.

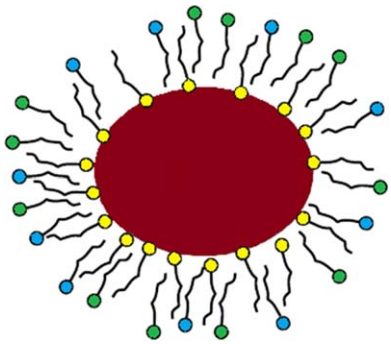

Figure 1. Nanoparticle stabilized by surfactant double layer: the first layer consists of oleic acid molecules (yellow 'heads'); the second layer consists of statistically distributed molecules of lauric acid and sodium dodecyl sulfate (green and blue 'heads').

For preparation of the *Ferrofluid 1*, 0.3 g of oleic acid was added to the reaction mixture before the hydrothermal treatment. A paste-like precipitate of barium hexaferrite was washed and easily peptized in hydrocarbons. A stable ferrofluid containing 'small' hexaferrite particles was obtained (*Ferrofluid 1*).

For preparation of the *Ferrofluids 2* and *3* the surfactant was added after hydrothermal treatment. Upon centrifuging, barium hexaferrite precipitate was suspended in a 1–2% aqueous ammonia solution, and then 0.1 g of oleic acid was added. The mixture was heated at stirring, until the acid was completely dissolved, and boiled for 10 min to remove excessive ammonia. 1 M hydrochloric acid was added until pH ≈ 3 was achieved. The paste-like precipitate, containing coated particles and excessive oleic acid, was separated, washed with deionized water, and dried in an oven at 105 °C.

The paste was suspended in a portion of *n*-octane and boiled for better surfactant adsorption. After the solvent was removed, the precipitate was washed from excessive acid with ethyl acetate. The separated precipitate was dried and peptized in petroleum ether. So, 'small' particles were transferred into a colloid (*Ferrofluid 2*), and the 'large' fraction coagulated and settled down.

In present study, an additional surfactant was empirically selected for a colloid, containing the 'large' nanoparticles (*Ferrofluid 3*), could be obtained.

The surfactant mixture contained equimolar amounts of sodium dodecyl sulfate (SDS) and lauric acid (LA). SDS was dissolved in water, solution was heated to 50 °C and LA was added at stirring. As a result, an emulsion, stable upon cooling to 20 °C, was obtained. The emulsion peptizes 'large' hydrophobic nanoplates due to the second surfactant layer with hydrophilic groups at the interface with the aqueous medium; as a result, non-transparent stable *Ferrofluid 3* is obtained. In Figure 1 the schematic view of the particle stabilized by a double layer of the surfactants is presented. Hydrocarbon tails are depicted as black curved lines and polar end groups as circles—yellow in case of oleic acid in the first layer, blue and green—SDS and LA. Polar groups at the surface make the particles lyophilic, so an aqueous colloid can be prepared.

The ferrofluids, based on cobalt (*Ferrofluid 4*) and copper (*Ferrofluid 5*) ferrite particles, stabilized by a double layer of surfactants, were prepared according to the procedure, described for *Ferrofluid 3*.

2.4. Instruments and methods for characterization of ferrite nanoparticles and ferrofluids

The physical properties and structure of ferrite nanoparticles were characterized by various techniques. The phase purity and crystal structure of the ferrite nanoparticles were examined using a Shimadzu XRD-7000 diffractometer with CuK_{α} radiation ($\lambda_{av} = 1.541\,84$ Å). The diffraction patterns were recorded in the 2θ range of 10°–80° in a step scan mode (step size—0.01°–0.005°; accumulation time—1.5–2 s).To identify the structure of ferrites, the JSPDS database was used. The morphologies of ferrite nanoparticles were observed using a JOEL JEM2100F transmission electron microscope. The content of metal ions in acidic ferrite solutions was determined using a Thermo Scientific iCE 3500 atomic absorption spectrometer with flame atomization. Each sample for transmission electron microscopy (TEM) was prepared by making a suspension of the ferrite powder in deionized water. The particle size of the sampled nanoparticles was determined by the mean linear intercept, which was acquired from TEM micrographs. Particle size in case of cobalt ferrite was determined by magnetic granulometry using a device designed in the Institute of Continuous Media Mechanics (Perm, Russia), described in [19].

Some methods were used for characterization of the particles in a colloid and in magneto-optical measurements the response of a colloid was registered.

An average hydrodynamic diameter and particle size distribution were determined by the dynamic light scattering (DLS) method using a Brookhaven ZetaPALS analyzer.

Magneto-optical measurements were carried out using a device designed in the Institute of Continuous Media Mechanics (Perm, Russia) and described in 'Results and Discussion' section.

The *Ferrofluid 3*, containing 'large' barium hexaferrite nanoplates, was studied by small-angle x-ray scattering (SAXS) and small-angle neutron scattering (SANS).

SAXS measurements were carried out using a Rigaku instrument with a rotating Cu-anode for two sample positions [20]. SANS measurements were performed using the two detector mode YUMO spectrometer in function at the 4th IBR-2 reactor neutron beamline [21, 22].

In the SAXS experiment, the samples of colloid were introduced into a capillary cell and in the SANS - into a Helma cell, the path way being 1 mm in both cases.

Initial data on small-angle diffraction were processed using a Rigaku software for SAXS and SAS software in a two-detector system mode for SANS [23].

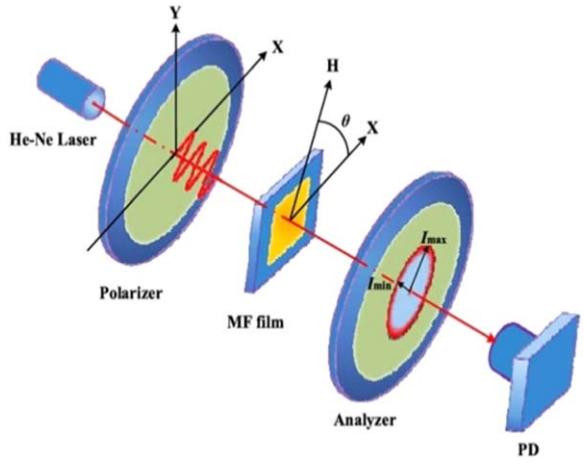

Figure 2. General scheme of light birefrigence—the beam is split into two orthogonally polarized rays with angle θ between them.

3. Results and discussion

3.1. Theoretical description of magnetic-optical phenomenon in ferrofluids

In physical optics, the Cotton–Mouton effect refers to birefringence in a liquid in the presence of a constant transverse magnetic field [24].

This effect arises due to constant magnetic moment of a molecule, which becomes oriented when the medium is subjected to magnetic field. In this case birefrigence can be registered, though its value is low enough for practical application in optical devices. Similarly, in a magnetic colloid, the moments of both spherical and anisometric particles are oriented along applied field. A uniaxial optical anisotropy appears in ferrofluids in magnetic field, either due to the orientation of anisometric dipole particles in an external field, or because of the reversible formation of chain aggregates composed of spherical particles and oriented along the field [25]. An anisotropy arising in magnetic fluid subjected to magnetic field results in splitting of the beam into two beams, like in anisotropic crystals. After the beam passes through the sample, elliptically polarized light is registered. The magneto-optical medium becomes birefringent and dichroic with respect to a passing optical beam: the refractive index and the absorption coefficient of this medium depend on the angle between the plane of polarization and optical axis, coinciding with the direction of magnetic field.

In alternating magnetic field at some constant amplitude, pronounced birefringence can be observed only if the frequency of magnetic field is lower than or comparable with characteristic frequency of Brownian rotation of the particle.

The optical anisotropy of a sample in an alternating magnetic field is proportional to the degree of particle orientation, similarly to magnetic susceptibility [26]. Consequently, the frequency dependence of the magneto-optical effects can be described by the same function with a correction taking into account the particle shape. When a linearly polarized wave propagates perpendicular to magnetic field, it can become elliptized. General scheme of light birefrigence is shown in Figure 2. Here the beam passing through the layer of magnetic fluid is split into two orthogonally polarized rays with a phase shift angle θ between them. Optical response is proportional to the intensity and phase shift of the beams.

In a colloid, optical response is proportional to the particle orientation degree, similar to magnetic susceptibility [27]. According to Debye law, the dependence of ferrofluid magnetic susceptibility on magnetic field frequency at constant field amplitude is expressed as:

$$\chi = \chi_0 / \left(1 + \left(\frac{f}{f_0}\right)^2\right), \tag{1}$$

where χ—magnetic susceptibility; χ_0—magnetic susceptibility in a constant field; f—frequency of applied magnetic field, f_0—characteristic frequency.

Hence, in case of magnetooptical media, susceptibility χ in Debye equation (1) can be substituted by the value of optical response, measured at a photodiode:

$$U_a = U_0 / \left(1 + \left(\frac{f}{f_0}\right)^2\right). \tag{2}$$

Here U_0 is response at constant magnetic field registered in the device, i.e. it is a combined characteristic of a device and a sample; f—frequency of applied magnetic field, f_0—characteristic frequency.

The value f_0, characteristic frequency, depends on the time of the Brownian rotation of the particles τ_B:

$$f_0 = 1/2\pi\tau_B. \tag{3}$$

From characteristic frequency, characteristic time of Brownian rotation of the particles in a colloid can be calculated by the formula:

$$\tau_B = 3\eta V/kT, \tag{4}$$

where η—viscosity of the medium; V—hydrodynamic volume of the particle; k—Boltzmann constant; T—absolute temperature.

In experiment, approximation of magneto-optical curve by Debye function (equation (2)) gives the value of characteristic frequency (equation (3)). If we know viscosity of the medium, hydrodynamic volume of the particle coated by a stabilizing layer, and, hence, particle size or diameter can be calculated (equation (4)).

Taking into account the concepts and phenomena given above, the following conclusion seems to be rather evident. The optical anisotropy of magnetic fluids with anisometric particles, nanorods or nanoplates, should be much more pronounced, than the one in the media with isometric particles. In other words, the magneto-optical effects will be substantially more sensitive to an applied magnetic field, or a less concentrated magnetic fluid can be used to obtain the same effect. This is important because of the strong absorption by magnetic particles in the optical spectral range.

The idea was to enhance the birefringence signal of a ferrofluid, using anisometric particles with the highest possible dimension ratio, in case of nanoplates it is the ratio of platelet diameter to its thickness. For such ferrofluids at low

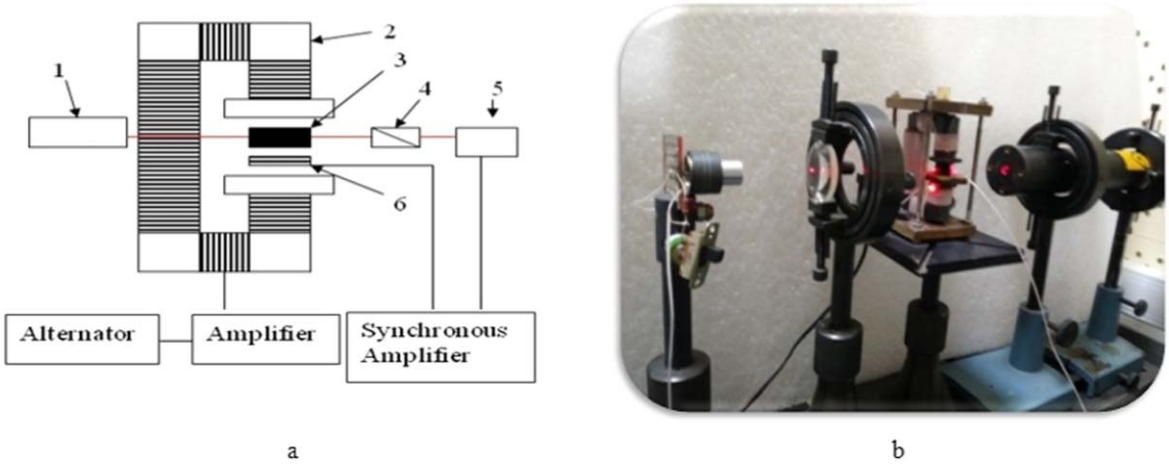

Figure 3. Magnetooptical device: scheme (a) and photo (b). In the scheme:1-helium-neon laser; 2-electromagnet with ferrite core; 3-sample cuvette; 4-analyzer; 5-photodiode; 6-magnetic field measuring coil.

concentrations the origin of magnetic induced birefringence can be explained by the only dominating factor—shape anisotropy of nanocrystallites.

3.2. Magneto-optical device

Magneto-optical measurements were carried out using a device designed by the authors. The photo and general scheme of the device are shown in figure 3. A cuvette with a sample is placed between the poles of a magnet producing vertically directed alternating magnetic field. A beam from helium-neon laser ($\lambda = 633$ nm) passes through the cuvette and polarizer-analyzer, installed at the angle 90° to the laser beam polarization plane, and then falls on a photodiode. The incident beam flux on the photodiode results in the photodiode generating output voltage. The angle between the polarization plane of the laser beam and the principal plane of the optical system is 45°. The distance that light travels through a ferrofluid layer, or the path length, is 8 mm. The beam passing through a birefringent medium becomes elliptically polarized [24].

At the photodiode, mounted next to the polarizer, intensity I of the transverse component of the elliptically polarized beam is registered. This value is connected with the phase difference φ between the ordinary and extraordinary beams:

$$I = (1 - \cos \varphi)/2. \quad (5)$$

For magnetooptical measurements the ferrofluids were diluted by the solvent until the registered intensity of the light passing through the cuvette was 30% of initial one.

The amplitude of magnetic field was 2 kA m^{-1} (~25 Oe).

3.3. Characterization of nanoparticles

The size of ferrite nanoparticles was determined by different methods. SEM-images of barium hexaferrite 'large' particles and copper ferrite nanoplates are presented in Figures 4 and 5, respectively. A plate-like irregular shape of the particles and the size of the order of 100 nm is clearly seen in both cases. In these ferrofluids, containing 'large' particles, it was possible to obtain the data using a light scattering device. In case of small particles, less than 10 nm, as in *Ferrofluids 1* and *4* ('small' particles of barium hexaferrite and cobalt ferrite) DLS device could not be used due to the particle size below the detection limit. Particle size distribution curves are shown in Figure 6. The Brownian translation diffusion time,

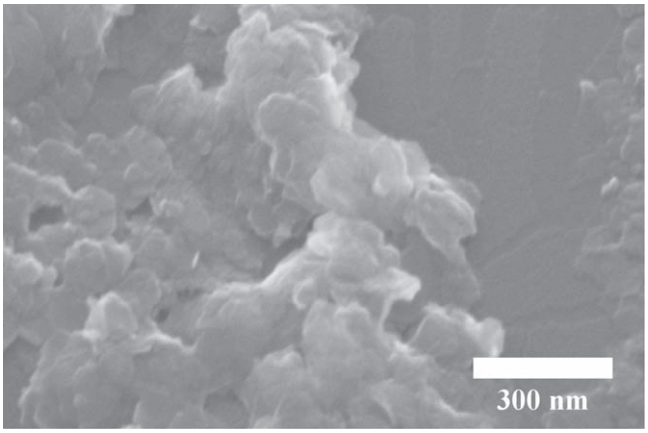

Figure 4. SEM-image of barium hexaferrite nanoplates.

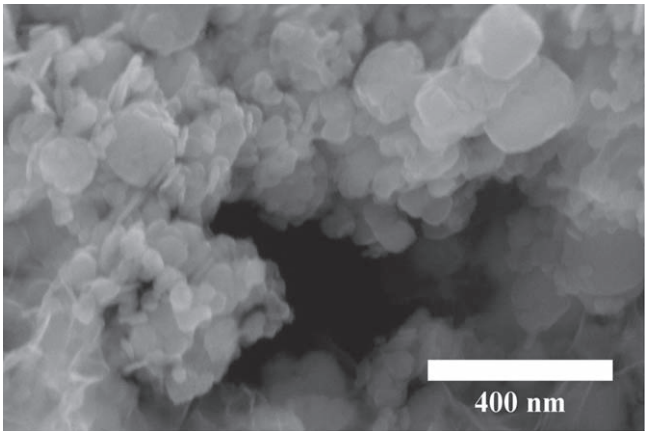

Figure 5. SEM-image of copper ferrite nanoplates.

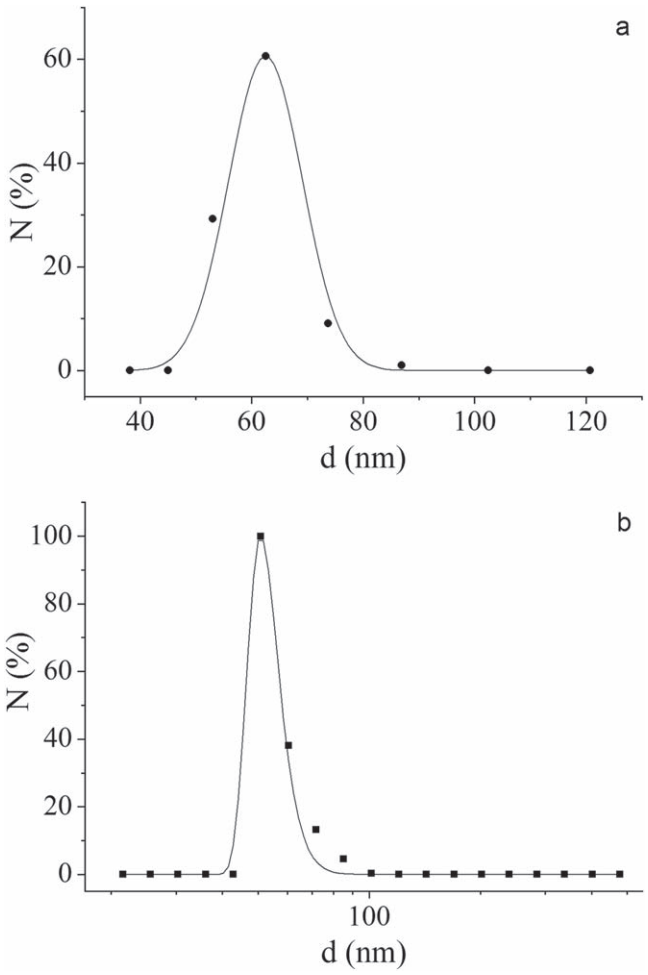

Figure 6. Particle size distribution in barium hexaferrite (a) and copper ferrite (b) colloids with 'large' nanoplates according to DLS data.

registered by the DLS method, is higher than the characteristic time of Brownian rotation τ_B, and diffusion of nanoplates and nanospheres of equal diameter can be considered to be identical processes.

The prevailing hydrodynamic diameter of barium hexaferrite (Figure 6(a)) and copper ferrite (Figure 6(b)) particles, calculated from the DLS data, is 61 and 51 nm, respectively. The values are consistent with the particle size seen on SEM-images (Figures 4 and 5).

For preparation of copper and cobalt ferrites, a novel synthetic method, developed by the authors, was used. So, additional analytical method was used for identification of these substances. From the data on metal content, obtained by atomic absorption spectroscopy, the formulas of ferrites were calculated. For cobalt ferrite it is close to stoichiometric-$Co_{0.92}Fe_2O_4$, and content of copper in copper ferrite is much lower than stoichiometric-$Cu_{0.65}Fe_2O_4$. The particle size of cobalt ferrite, determined from magnetization curve, was about 9 nm. Unlike DLS, in this method the size of magnetic core is determined, and for hydrodynamic particle size the stabilizing layer thickness can be calculated [28] from atomic bonds given in reference books.

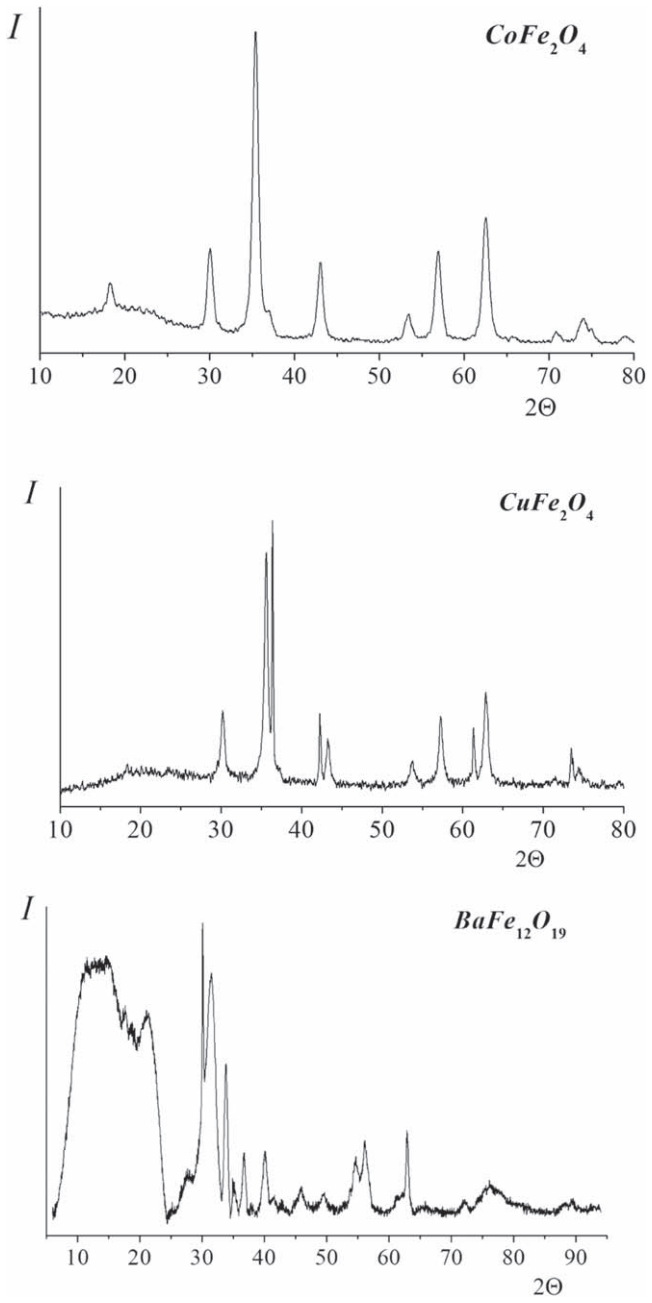

Figure 7. X-ray diffraction patterns for cobalt ferrite, copper ferrite, barium hexaferrite.

Crystalline structure of ferrite nanoparticles was studied by X-ray diffraction method. Diffraction patterns of the samples are given in Figures 7(a)–(c). A single phase diffraction pattern can usually be readily identified by searching a data base of reference powder patterns, so the standard cards were selected. It should be noted that no complete incidence of the patterns and cards is observed due to the structure with some sites of divalent metal, substituted by iron. However, the main intense peaks of the diffraction patterns, shown in Figures 7(a), (b), correspond to the ASTM 00-003-0864 card (cobalt ferrite) and ASTM 00-025-0283 card (copper ferrite).

In Figure 7(c), the X-ray pattern of $BaFe_{12}O_{19}$ nanoparticles is given, most intensive diffraction peaks from ICDD

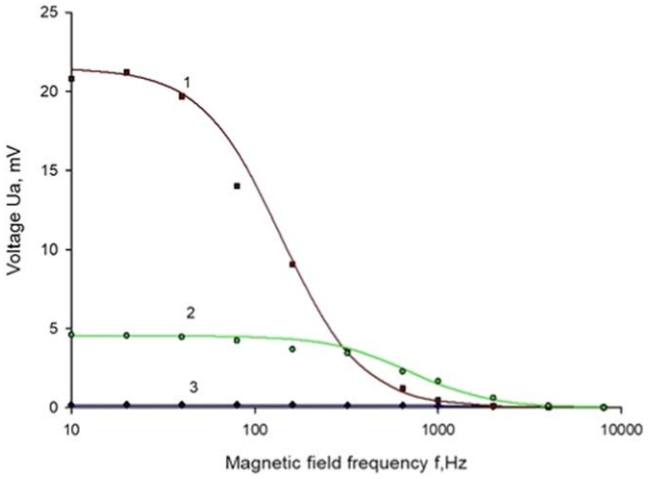

Figure 8. Frequency characteristics of magnetic optical signal for ferrofluids: (1)-*Ferrofluid 3*, 'large' nanoplates, $BaFe_{12}O_{19}/H_2O$; (2)-*Ferrofluid 5*, 'large' nanoplates, $Cu_{0.64}Fe_2O_4/H_2O$; (3)-*Ferrofluid 2*, 'small' nanoplates, $BaFe_{12}O_{19}$ /$C_{11}H_{24}$.

98-006-0984 card coincide with experimental diffraction peaks. It means that the XRD pattern has a hexagonal structure. However, magnitudes of diffraction peaks intensities mismatch with ICDD. This fact can be explained by a high-level imperfection of the unit cells.

3.4. Magneto-optical properties of ferrofluids

3.4.1. Ferrofluid 1. In the *Ferrofluid 1* barium hexaferrite particles were dispersed in a hydrocarbon medium. It was prepared via the first variant of hydrothermal procedure, i.e. oleic acid was added before autoclaving. The diameter of nanoplates was 8 nm and thickness—3 nm [17]. Weak magnetism of these particles can be explained by the thickness of two nonmagnetic layers on the nanoplate surfaces—1.6 nm in total. Subtracting this value from the particle thickness (3 nm), we obtain too thin magnetic core. So, no measurable signal was observed at magneto-optical measurements of this ferrofluid due to very small magnetic moment of the particles.

3.4.2. Ferrofluid 2. For magneto-optical measurements, a hydrocarbon colloid, obtained upon dispersing of hydrophobized 'large' barium hexaferrite particles in petroleum ether (*Ferrofluid 2*) was diluted with undecane. Petroleum ether was evaporated, so viscosity of the medium (undecane) was close to 1 mPa s. A low voltage value, registered at the photodiode (Figure 8-(3)), was twofold higher than the one observed in case of the *Ferrofluid 4* (cobalt ferrite). The approximation gives $f_0 = 185$ Hz and $d = 61$ nm. This particle diameter is equal to the average diameter of 'large' barium hexaferrite nanoplates obtained by the DLS method. Deviation of the experimental data from the approximating curve is considered to be due to a wide particle size distribution. Probably, main fraction in *Ferrofluid 2* is weakly magnetic 'small' particles. This fraction gives no contribution to the magneto-optical effect. Some amount of nanoplates with diameter of ~60 nm, or 'large' particles, are transferred into a colloid, and optical anisotropy arises. In figure 8 the curves of frequency characteristics of magnetic optical signal for 3 ferrofluids are given. Obviously, the intensity of the magneto-optical response depends both on the shape and size of the particles.

3.4.3. Ferrofluid 3.. In figure 9 the photo of synthesized aqueous magnetic colloid containing 'large' barium hexaferrite nanoplates (Figure 9(a)) is presented with the schematic picture explaining behavior of the particles in initial ferrofluid (Figure 9(b)) and when subjected to magnetic field (Figure 9(c)). In the field the multidirectional magnetic moments of particles become oriented parallel to the applied field [29].

As it was expected, for the 'large' barium hexaferrite nanoplates (*Ferrofluid 3*), the maximum value of the magneto-optical response was found to be two orders of magnitude higher than that in case of *Ferrofluid 2* (Figure 8-(1)). Excellent fitting of experimental points of the frequency dependence with approximating curve indicated particle size distribution to be rather narrow. In this case the parameters, determined from the curve were: $f_0 = 140$ Hz, $d = 144$ nm. So, calculated diameter is more than 2 times higher than the average hydrodynamic diameter determined by the DLS method (61 nm). This can be explained by a strong dilution in DLS measurements—colloidal solutions with particle concentration of $\sim 2 \times 10^{-3}$ vol% are used, whereas in magneto-optical measurements, the concentration is two orders of magnitude higher. Probably, an equilibrium aggregation of rather coarse colloid particles is observed in these samples, which leads to a larger effective size in magneto-optical measurements. A slow sedimentation is also observed in these colloids, which is also due to the particle aggregation, because separate particles less than 500 nm in size cannot settle down due to the thermal movement [30]. At a stronger dilution (DLS), the aggregates dissociate and we observe the diffusion of individual particles and determine just their size.

In [31] absorption of light by ellipsoid-shaped particles is analyzed. Besides, the influence of magnetic field on the absorption and, hence, transmission, is evaluated. In present study, for comparison of magneto-optical response to be correct, the samples were diluted until the intensity of transmitted light was 30% from the one of incident light. In general, absorption and scattering decrease intensity of transmitted light and magneto-optical response. The dependence of transmittance on these phenomena in *Ferrofluid 3* was estimated and relative transmittance as a function of frequency was built (Figure 10). In our experiments polarization of light was found to be the only dominating reason of magneto-optical phenomenon. It was shown, that the contribution of absorption and scattering can be neglected.

3.4.4. Ferrofluid 4. The registered optical signal for cobalt ferrite (*Ferrofluid 4*) was negligibly low, the values being about the sensitivity limit of the device. The approximation of

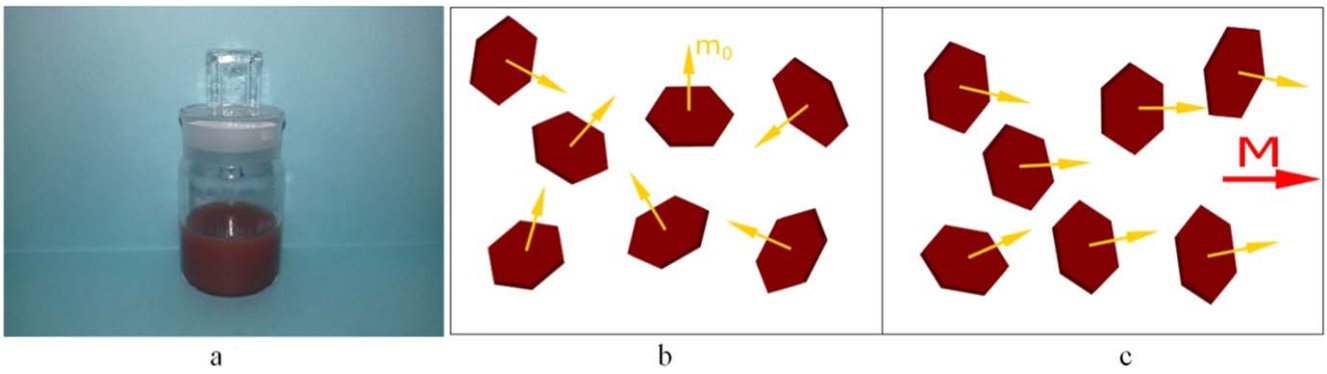

Figure 9. Synthesized aqueous magnetic colloid containing 'big' barium hexaferrite nanoplates (a); initial particles with multidirectional magnetic moments (b); nanoplates with the moments parallel to the applied magnetic field (c).

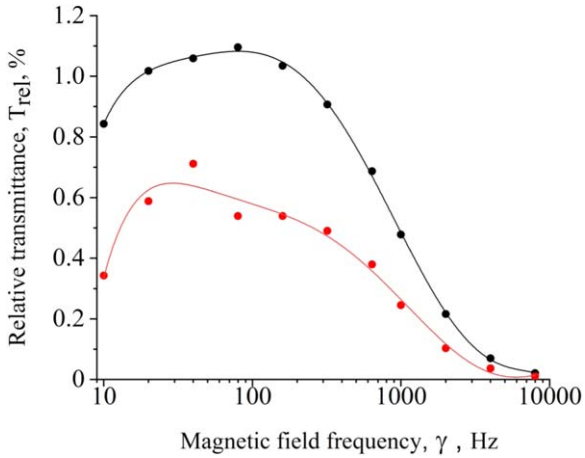

Figure 10. Dependence of relative transmittance on magnetic field frequency for *Ferrofluid 3*.

the data by Debye function (equation (2)) gave the values $f_0 = 290$ Hz and $d = 113$ nm. In this case magneto-optical effect is likely to be due to anisometric aggregates present at a low concentration, spherical colloid particles make no contribution to optical anisotropy. In [32], electrostatic stabilization of $CoFe_2O_4$ was carried out, and agglomeration was not pronounced. The presence of small aggregates (~27 nm) at relatively high concentration resulted in a noticeable magneto-optical effect.

3.4.5. Ferrofluid 5. *Ferrofluid* 5, an aqueous copper ferrite colloid, demonstrated a considerable magneto-optical response (figure 8-(2)). The shape and size of the particles is quite similar to the ones in *Ferrofluid 3*. So, these ferrofluids can be compared, though, according to the reference books, magnetic properties of the bulk substances are different. The particle size of 84 nm determined using magneto-optical data, is much closer to the one, determined by DLS (51 nm), than in case of *Ferrofluid 3*. This means the aggregation degree is much lower. The absorbance of copper ferrite in red spectral region is higher than the one of barium hexaferrite, so concentration in the sample transmitting 30% of the beam, prepared for the measurements, is lower. This can be a reason for a weaker magneto-optical response. The value of characteristic frequency for *Ferrofluid 5* is 700 Hz (compare with 140 for *Ferrofluid 3*). It is known, that the higher is the frequency, the faster is the response of a magneto-optical sensor. Additional experiments should be carried out for amount of the solvent and precise concentration value to be taken into account.

3.4.6. Comparison of magneto-optical properties of ferrofluids. The data on characteristic frequency and particle size in different ferrite colloids are given in table 1. In this table both results obtained within the present research and literature data are summarized.

In general colloids with 'small' particles are characterized by a weak or negligible optical response and high characteristic frequency. Particle sizes calculated by the formula, in all cases are much bigger than the ones determined experimentally by different methods—transmission electron microscopy, magnetic granulometry, DLS—due to more or less pronounced tendency to aggregation. In our study the best result, or the highest value of magneto-optical response, was observed in the case of barium hexaferrite colloid, containing 'large' nanoplates. It should be noted, that there are some reasons explaining the difficulties connected with comparison and analysis of experimental data with the information given in literature. The first reason is the lack of information, for example, in [33] viscosity of the medium is omitted. In some cases the data and values, which can be calculated from magneto-optical curves, are lacking. In [32, 33], no data on characteristic frequency for cobalt ferrite colloid was found, so it could be visually determined from the curve very approximately. As a rule, there are some differences in design of magneto-optical devices and lacking data on magnetic field amplitude. However, general tendency can be traced, i.e. enhanced magneto-optical response and lower characteristic frequency values for the colloids with large anisometric particles or aggregates.

3.4.7. The study of the Ferrofluid 3 by SAXS and SANS methods. As the *Ferrofluid* 3 demonstrated the highest optical response when subjected to an alternating magnetic

Table 1. Characteristic frequency and particle size for ferrite colloids.

Ferrite	Characteristic frequency f_0, Hz	Calculated particle diameter d, nm	Particle size, nm
$BaFe_{12}O_{19}$, 'small' plates	No measurable magneto-optical response	—	8 × 3 (TEM)
Ferrofluid 1			
$BaFe_{12}O_{19}$, 'small' isolated from 'large'	1850	61	Low fraction of 'large'
Ferrofluid 2			
$BaFe_{12}O_{19}$, 'large' plates	140	144 (aggregates)	61 (DLS)
Ferrofluid 3			
$Co_{0.92}Fe_2O_4$, nanospheres	290	113 (aggregates)	9 (magnetic granulometry)
Ferrofluid 4			
$Cu_{0.64}Fe_2O_4$ nanoplates	700	84	51 (DLS)
Ferrofluid 5			
$CoFe_2O_4$ [26] nanospheres	~20 000	27 (chains)	~7 (TEM)
$CoFe_2O_4$ [27] nanospheres	~150	Chains	13 (core,TEM), 36 (core+shell, calculation)

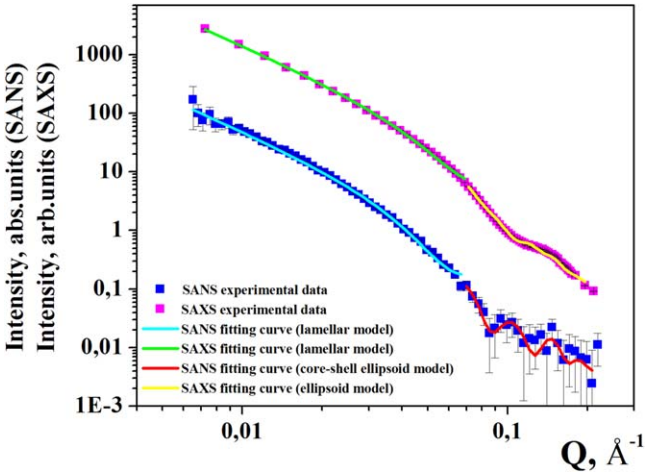

Figure 11. SANS and SAXS experimental and model fitting curves for *Ferrofluid 3*.

field, some additional methods were used for a detailed study of the stabilized nanoplates.

In Figure 10 the experimental SAXS and SANS curves from the sample composed of colloidal suspension of $BaFe_{12}O_{19}$ particles stabilized by a double layer surfactant in water are represented. The double layer consists of oleic acid (OA), the first layer, and SDS–LA, the second layer (figure 1).

In Figure 11 some curves are presented, where the scattering intensity is a function of the scattering vector is presented. Scattering vector is described by the following equation:

$$Q = \frac{4\pi}{\lambda} \sin \frac{\Theta}{2}, \tag{6}$$

where λ—the wavelength of incident X-rays or neutrons, θ—the scattering angle.

Using SASView [34] software for fitting the experimental curves, the following results were obtained (figure 11):

(i) *In the range of* $0.0072 < Q < 0.1$ Å^{-1}, the scattering intensity corresponds to dilute, randomly oriented sheets, 'infinitely large' in comparison with their thickness.

(ii) *In the range of* $0.1 < Q < 0.5$ Å^{-1}, scattering characteristic for dilute, randomly oriented particles of ellipsoidal form is detected.

The model fitting of the experimental curves, as well as the TEM image showed the system to be composed of a polydisperse mixture: (i) sheets, 'infinitely large' as compared to their thickness and (ii) ellipsoidal particles. In Figure 12 the parameters of a core–shell structure, given in Table 2, are illustrated.

The average thickness of the sheets is found to be about 7 nm according to SAXS data and about 8.8 nm according to SANS data. The difference between the thicknesses obtained by the two methods can be explained by their possibilities. The SAXS method is not sensitive to the surfactant. However, the surfactant layer can be detected by SANS. We can assume that the surfaces of the sheets are coated with a single surfactant layer, and at the edges—with a double layer (figure 13).

The average dimensions of the ellipsoidal particles obtained by means of SAXS and SANS methods are $2R_1 \sim 8$ nm and $2R_2 \sim 21$ nm. The thickness of the surfactant layer was obtained using SANS data, the values in equatorial and polar directions of the ellipsoid being different (figure 14).

From the SANS data, we conclude that two scenario of surfactant distribution on the nanoparticle surface can be possible:

(a) An uniform layer of OA on all the ellipsoidal particle surface and the second layer of SDS+LA on the elongated part of the particle;

(b) The layer of OA covers the elongated part of the particle; polar regions of the ellipsoidal particle are covered with a layer of SDS+LA surfactants; the

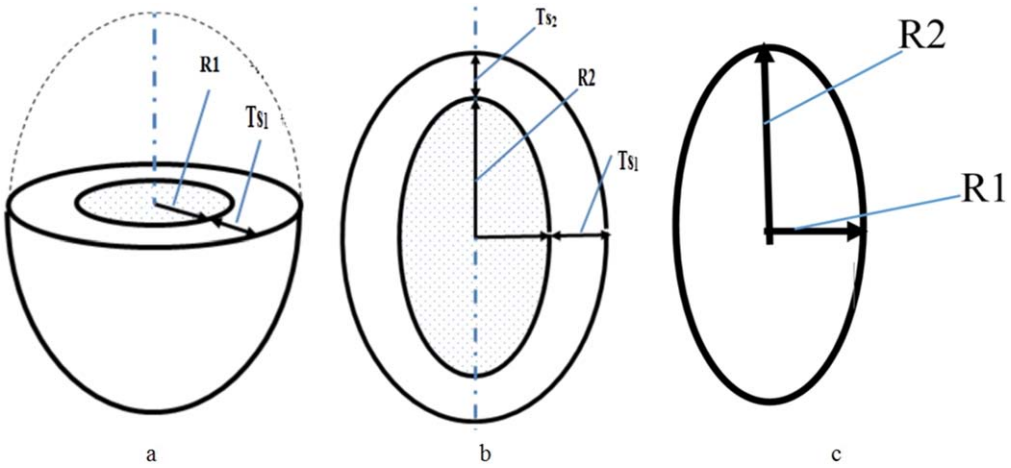

Figure 12. The description of the model parameters for core–shell ellipsoid (a), (b) and ellipsoid (c) models.

Table 2. Model parameters calculated from SANS and SAXS data.

Method	Q-range, Å^{-1}	Model	Model parameters	Model parameters values, nm
SANS	$0.0072 < Q < 0.07$	Sheets, 'infinitely large	Thickness	8.8 ± 0.2
	$0.07 < Q < 0.21$	Core–shell	R_1	3.9 ± 0.3
		Ellipsoid	R_2	10.8 ± 0.3
			Ts_1	4 ± 0.2
			Ts_2	1.5 ± 0.1
SAXS	$0.0072 < Q < 0.07$	Sheets, 'infinitely large	Thickness	7.2 ± 0.1
	$0.07 < Q < 0.21$	Ellipsoid	$R1$	3.7 ± 0.1
			$R2$	10.6 ± 0.1

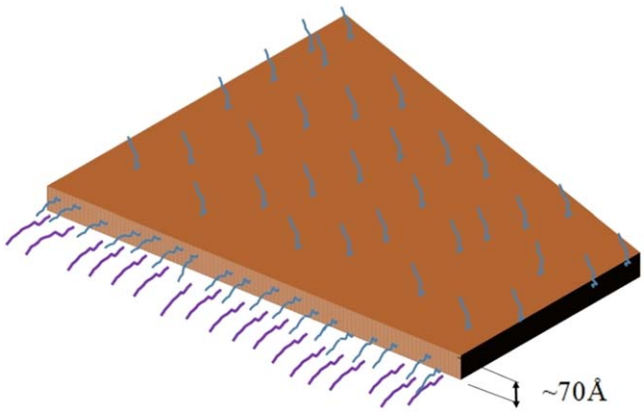

Figure 13. Schematic representation of an 'infinitely large' sheet particle.

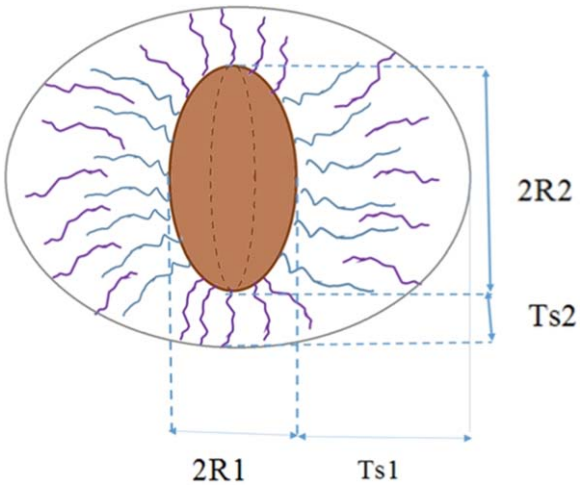

Figure 14. Schematic representation of possible distribution of surfactant molecules at the nanoparticle surface.

longitudinal edges of the particle are coated with a double layer of surfactants.

It can be concluded that SAXS and SANS results are consistent with particle sizes determined by TEM (Figure 15).

It is known that sizes in the range of $4 \div 5$ nm have special properties associated with the surface-to-volume ratio [35, 36]; therefore, the properties of the surfactant will be selective to the sizes of the stabilized particles. Thus, surfactants can be differently adsorbed on the surface of small particles and on the top and lateral surfaces of the sheets.

For more information it will be necessary to study the samples of particle dispersions in deuterated water by SANS.

3.4.8. The novelty of present study. Thus, the main finding of this study is an enhanced optical response of barium hexaferrite and copper ferrite colloids in an external magnetic field. This behavior is explained both by size and a high aspect ratio of nanoplates. From synthetic point of view, preparation of 'large' plate-like particles and colloids

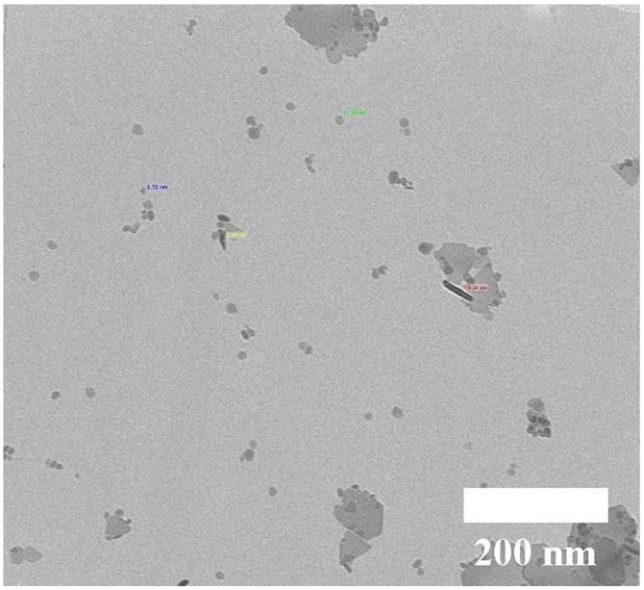

Figure 15. TEM-image of the particles in *Ferrofluid 3*.

containing these particles is a great achievement. In general, copper ferrite is less studied and information on the synthesis of nanoparticles is rather scarce. No data on copper ferrite nanoplates and magneto-optical response of copper ferrite colloids were found in literature. The magneto-optical signal in the samples of *Ferrofluid 3* and *5* was by orders higher than that of the ferrofluids with 'small' nanoparticles, both spherical and anisometric. Recently the authors have established some regularities and mechanism of particle stabilization in magnetic colloids [37]. In addition, the structure of the surface layer has been described [28]. In present work the mechanism of particle stabilization is not clear enough due to some contradictory data, obtained using SAXS and SANS methods. However, the idea of a double layer formation and its implementation in experiment was successful. Preparation of the ferrofluids containing 'large' particles became possible after a two-step coating procedure, which resulted in a double surfactant layer on the particle surface. It should be noted that stability of *Ferrofluid 5* containing copper ferrite nanoplates, is over two weeks, and in case of the *Ferrofluid 3* (barium hexaferrite) the concentration gradient, or beginning of sedimentation, can be visually observed in two days. So, further efforts should be directed to preparation of a more stable ferrofluid containing barium hexaferrite particles and more detailed study of magneto-optical properties, stabilizing mechanism and the role of particle aggregation.

4. Conclusion

Magnetic nanoplates of barium hexaferrite were synthesized by the hydrothermal method and aqueous colloids were prepared. Nanoparticles of magnetic cobalt and copper ferrites were synthesized via a novel method. For stabilization of the 'large' magnetic particles, a lyophilizing mixture of SDS and LA was experimentally selected. A double layer allowed aqueous ferrofluids, containing relatively large barium hexaferrite and copper ferrite particles, 61 and 51 nm respectively, to be obtained. The colloids containing barium hexaferrite nanoparticles were found to be stable over two days, and those with copper ferrite nanoparticles—over two weeks. The particle size of ferrites was determined by DLS method and electron scanning microscopy. The element content was determined by atomic absorption spectroscopy. Metal ferrites have also been studied using such methods as small angle x-ray scattering and small angle neutron scattering. Magneto-optical response in ferrofluids was found to be rather different. A pronounced magneto-optical effect was observed in aqueous colloid containing 'large' barium hexaferrite nanoplates. Hydrocarbon colloids containing 'small' barium hexaferrite nanoplates were characterized by a weak magneto-optical effect, the value being by two orders of magnitude lower than the one for the ferrofluid with 'large' particles. A colloid based on copper ferrite was also shown to be an efficient magneto-optical medium. Nevertheless, its response was about 5 times lower, than in case of 'large' barium hexaferrite nanoplates.

The characteristic frequencies f_0 were determined using experimental data and particle (aggregate) sizes were calculated. It was shown, that the aggregates consisting of 2–3 particles (144 nm), are present in barium hexaferrite colloid. In case of copper ferrite colloid, aggregation degree is lower —according the calculations from magneto-optical data, aggregate size is 85 nm, i.e. only two-particle aggregates are present.

The results of SAXS and SANS on particle size were consistent with microscopic and DLS data. However, the structure of a stabilizing layer and stabilization mechanism are not still quite clear due to some contradictory results of SAXS and SANS data treatment.

Thus, it was demonstrated, that in the media with equal viscosity magneto-optical response largely depends both on particle geometry and magnetic properties of the substance. In future the magneto-optical media will be studied using the light sources with different wavelengths. Further research, connected with the synthesis and stabilization of magnetic fluids with anisometric particles and optical response of these media will contribute to the development of new technologies and theoretical concepts. New ferrofluids with enhanced magneto-optical response are also expected to find new application areas.

Acknowledgments

The study was financially supported by the Government of Perm Krai, the research project no. S-26/791.

This work benefited from the use of the SasViewapplication, originally developed under NSF award DMR-0520547. SasView contains code developed with funding from the European Union's Horizon 2020 research and innovation programme under the SINE2020 project, grant agreement No. 654000.

The authors are grateful to A I Nechaev for assistance in DLS experiments.

ORCID iDs

S A Astaf'eva https://orcid.org/0000-0003-2018-2908
V A Turchenko https://orcid.org/0000-0002-4755-3898

References

[1] Kefeni K K, Msagati T A M and Mamba B B 2017 *Mater. Sci. Eng.* B **215** 37–55
[2] Phumying S, Labuayai S, Swatsitang E, Amornkitbamrung V and Maensiri S 2013 *Mater. Res. Bull.* **48** 2060–5
[3] Sasaki T *et al* 2010 *J. Supercrit. Fluids* **53** 92–4
[4] Ito A, Shinkai M, Honda H and Kobayash T 2005 *J. Biosci. Bioeng.* **100** 1
[5] Haun J B, Yoon T-J, Lee H and Weissleder R 2010 *Wiley Interdiscip. Rev. Nanomed. Nanobiotechnol.* **2** 291
[6] Amblard F, Yurke B, Pargellis A and Leibler S 1996 *Rev. Sci. Instrum.* **67** 818
[7] Bausch A R, Ziemann F, Boulbitch A A, Jacobson K and Sackmann E 1998 *Biophys. J.* **75** 2038
[8] MacKintosh F C and Schmidt C F 1999 *Curr. Op. Coll. Interf. Sci.* **4** 300
[9] Cheieh J J *et al* 2005 *J. Appl. Phys.* **97** 043104
[10] Deng H *et al* 2008 *Appl. Phys. Lett.* **92** 233103
[11] Liu T *et al* 2007 *Appl. Phys. Lett.* **91** 121116
[12] Yang S Y *et al* 2004 *Appl. Phys. Lett.* **84** 5204–6
[13] Yerin C V 2017 *J. Magn. Magn. Mater.* **431** 27–9
[14] Verma S, Joy P A, Khollam Y B, Potdar H S and Deshpande S B 2004 *Mater. Lett.* **58** 1092–5
[15] Lodhi M Y *et al* 2014 *Curr. Appl Phys.* **14** 716–20
[16] Desai I *et al* 2019 *Mat. Sci. Energy Technol.* **2** 150–160
[17] Primc D, Makovec D, Lisjak D and Drofenik M 2009 *Nanotechnolgy* **20** 1–9
[18] Makovec D, Primc D, Sturm S, Kodre A, Hanzel D and Drofenik M 2012 *J. Solid State Chem.* **196** 63–71
[19] Pshenichnikov A F, Mekhonoshin V V and Lebedev A V 1996 *J. Magn. Magn. Mater.* **161** 94–102
[20] Kuklin A I *et al* 2012 *J. Phys.: Conf. Ser.* **351** 012009
[21] Kuklin A I, Islamov A K and Gordeliy V I 2005 *Neutron News* **16–3** 16–8
[22] Kuklin A I *et al* 2018 *J. Phys.: Conf. Ser.* **994** 012016
[23] Soloviev A G, Solovjeva T M, Ivankov O I, Soloviov D V, Rogachev A V and Kuklin A I 2017 *J. Phys.: Conf. Ser.* **848** 012020
[24] Landsberg G S 1976 *Optika (Optics)* (Moscow: Nauka) p 926
[25] Hasmonay E, Dubois E, Bacri J C, Perzynski R, Raikher Y L and Stepanov V I 1998 *Eur. Phys. J.* B **5** 859–67
[26] Chung S H, Hoffmann A, Gusliyenko K, Bader S D, Liu C, Kay B, Makowski L and Chen L 2005 *J. Appl. Phys.* **97** 10R101
[27] Connolly J and St Pierre T G 2001 *J. Magn. Magn. Mater.* **225** 156–60
[28] Lysenko S N, Derechi K A, Astaf'eva S A and Yakusheva D E 2018 *Inorg. Mater. Appl. Res.* **9** 334–42
[29] Mertelj A and Lisjak D 2017 *Liq. Cryst. Rev.* **5** 1–33
[30] Otterstedt J-E and Brandreth D A 1998 *Small Particles Technology* (New York: Springer Science+Business Media) p 519 978-1-4757-6523-6
[31] Sanz-Felipe Á and Martín J C 2018 *J. Phys. D: Appl. Phys.* **51** 135001
[32] Jamon D, Donatini F, Siblini A and Royer F 2009 *J. Magn. Magn. Mater.* **321** 1148–54
[33] Chung S-H *et al* 2008 *J. Magn. Magn. Mater.* **320** 91–5
[34] Doucet M *et al* 2017 SasView version 4.1.2., Zenododoi.org/10.5281/zenodo.825675
[35] Avdeev M V *et al* 2007 *J. Magn. Magn. Mater.* **311** 6–9
[36] Kuklin A I *et al* 2011 *Rom. J. Phys* **56** 134–40 http://www.nipne.ro/rjp/2011_56_1-2/0134_0141.pdf
[37] Lysenko S N, Astaf'eva S A, Yakusheva D E and Balasoiu M 2019 *Appl. Surf. Sci.* **463** 217–26